International Journal of GEOMATE, Nov., 2017, Vol.13, Issue 39, pp.198-205
Geotec., Const. Mat. and Env., ISSN:2186-2990, Japan, DOI: https://doi.org/10.21660/2017.39.65526

CORROSION DAMAGE MEASUREMENT ON REINFORCED CONCRETE BY IMPRESSED VOLTAGE TECHNIQUE AND GRAVIMETRIC METHOD

Emel Ken Benito[1], Marish S. Madlangbayan[2*], Nimfa Maren S. Tabucal[2], Marloe B. Sundo[2], and Perlie P. Velasco[2]

[1]Corporate Development Engineer, Cumberland Development Corporation, Philippines; [2]Faculty, University of the Philippines, Los Baños, Laguna, Philippines

*Corresponding Author, Received: 16 July 2017, Revised: 14 August 2017, Accepted: 25 August 2017

ABSTRACT: This study investigated the effect of sea water on the corrosion behavior of reinforcing steel in concrete. A 3% sodium chloride solution was used to simulate sea water. The solution was used as mixing water as well as immersion media. Combinations of mixing and immersion media considered in this study were normal-normal water (NN), normal-sea water (NS), seawater-normal water (SN), and seawater-seawater (SS). Corrosion measurement used were Impressed Voltage Test (IVT) and gravimetric method. Results showed that corrosion current curves, gravimetric mass loss, the average and maximum current passed are severe in SS but negligible in NN. The difference between NS and SN, however, is not well defined but was shown to differ in terms of corrosion current behavior before and after cracking. Incorporating chloride in the mix, regardless of its environment, was found to cause rapid crack development in concrete. Statistical analysis suggested that the presence of chloride had no influence on the outcome of percent mass loss with respect to the control sample except in SS combination.

Keywords: Reinforced concrete, Corrosion damage, Impressed voltage test, Chloride penetration

1. INTRODUCTION

Corrosion presents a worldwide issue because of the increased risk of failure in reinforced concrete (RC) structures, and the high cost to maintain and repair these structures. Chloride attack has been known to participate in the process and is primarily attributed for spalling and cracking in concrete [1].

Chloride plays an indirect role in steel corrosion. At an alkalinity level normally present in concrete, a thin lime-rich passivating layer is formed at steel-concrete interface which acts as “alkaline buffer”, rendering the steel surface passive [2]. The structure and ways by which the film degrades under aggressive conditions are currently the subject of research. It is well understood, however, that chloride displaces some of the oxygen in the layer, creating a porous and conductive oxide film.

Chloride can exist in concrete by virtue of airborne sea water particulates. These particulates were reported to travel 2 km or farther, depending on wind profile and topography [3]. While current standards and building codes, such as ASTM C 160 and ACI 222, would set the permissible chloride content in concrete mixing applications, the role of sea water in concrete corrosion is still not well understood. Some would argue that there are successful cases of mixing seawater in concrete under marine environment [4]. There were also reports pointing to the influence of chloride-contaminated mixing and immersion medium to concrete corrosion [5]. However, the extent of damage incurred by the aggressive environment has not been actually quantified. Many researchers in recent years has shifted their attention towards surface penetration technique with cementitious materials such as silica to reduce the penetration rate of contaminants that may degrade the quality of the concrete [6].

Since corrosion is a very slow process, electrochemical techniques have long been used to reduce the time of rebar depassivation to a desirable time-scale. One of which is Impressed Voltage Test (IVT). In this method, rapid corrosion is facilitated by raising the potential difference between two electrochemical sites. The amount of mass consumed is directly related to the flow of electrical energy which can be modelled by Faraday’s law [7]. Much of the available studies would focus on applying aggressive electrolyte, such as chloride, to amplify the actual damage when introducing inhibiting materials in concrete [8]. For an accelerated process, however, the result is very conservative. It is worthy to note that even as Impressed Voltage Method is common, no work has been found describing the efficiency of the method

to describe the said observation.

Given the current research gaps, impressed voltage technique was used to facilitate rapid corrosion in sodium chloride concentration generally present in sea water (3% by weight). Corrosion activity was also facilitated by IVT in a solution free of chloride. To quantify the loss of weight in corrosion, Faraday's law and gravimetric methods were employed.

The present research explores the potential use of sea water in RC structures with respect to concrete durability and reinforcement corrosion. The result that can be obtained from the study is of utmost importance when potable water supply offshore may be limited for concrete-based construction. The primary advantage of this study is that by using IVT, the damage in terms of mass loss can be quantified, and the time of corrosion development is so rapid that concrete cracking can be observed in a matter of days. Thus, the effect becomes more controlled and pronounced.

The general objective of this study is to investigate the corrosive effect of sea water in RC exposed to fresh and brackish water. Specifically, this study aims to:

1) Determine the extent of corrosion in terms of mass loss in reinforcing bars under fresh water using IVT and weight loss analysis.

2) Determine the extent of corrosion in terms of mass loss in reinforcing bars under marine environment using IVT and weight loss analysis.

3) Compare the corrosion behavior of chlorinated immersion and mixing medium in terms of electrochemical mass loss.

2. MATERIALS AND METHODS

The study was designed to test the applicability of seawater as mixing water subjected to fresh and seawater atmospheres under accelerated process.

2.1 Materials used

2.1.1. Cement

ASTM C 150 Type I Portland Cement was used as the binding material. This particular type of cement is commonly used for general building construction due to relatively high tricalcium aluminate (C3A) content, necessary for early strength development.

2.1.2 Aggregates

Fine aggregates were derived from crushed rocks (Sand S1). Standard laboratory experiment yielded a specific gravity of 2.50 and an average fineness modulus of 2.56. Gravel sieved at maximum particle size of 0.75 in (19 mm) was used as coarse aggregates, which has specific gravity of 2.67 and unit weight of 1,582 kg/m^3.

2.1.3 *Steel reinforcement and NaCl solution*

Rebar samples are Grade 33 deformed mild steel (PNS 49:2002) with 0.5-in. (12 mm) diameter, cut into 8-in. (200 mm) lengths. Commercially available rock salt was used to prepare the 3% salt water concentration by weight.

2.2. Mixture Proportion

A water-cement ratio (w/c) in concrete production of 0.55 was selected. Mix proportioning followed the method described in ACI 211 (Standard Practice for Selecting Proportions for Normal, Heavy-weight, and Mass Concrete). Two (2) setups have been prepared: one that is mixed with sea water, and a controlled test sample mixed with pure water. Each setup is to be immersed under water with or without 3% NaCl, summing to four (4) test scenarios. A total of 12 RC specimens have been prepared, making three (3) trial specimens allotted for each scenario. Mix proportioning of concrete are given in Table 1.

Table 1. Mix proportion of each concrete material for natural and chloride-contaminated setup

MATERIAL	WEIGHT	
	Natural[a] (kg/m³)	Seawater[b] (kg/m³)
Water	200.00	200.000
Cement	363.64	363.64
CA	1, 019.34	1, 019.34
Air	–	–
3% NaCl	–	6.19
FA	705.25	698.11
Total	2, 288.22	2, 279.27

[a] slump = 35 mm
[b] slump = 25 mm

2.3 Specimen Preparation and Testing

Prior to casting, workability of specimens was tested using slump test under ASTM C 143 standard. The test samples were then allowed to set under room temperature for 24 hours, and moist-cured for an additional 28 days in a water bath as per ASTM C 192. Impressed voltage technique was carried at the end of 28-day curing period.

2.3.1 NaCl solution

Chloride-contaminated water was prepared by mixing sea salt and purified water at 3% concentration by weight of solution.

2.3.2 Reinforced concrete specimen

Each rebar sample was weighed prior to casting using an analytical balance with precision of 0.01 g. A 4 in. x 8 in. (100 mm x 200 mm) cylindrical molds (in conformance to ASTM C 470) were used to cast the RC specimens. Bar samples have 2 in. (50 mm) protruded part resting at the same clear distance from the bottom, as shown in Fig. 1.

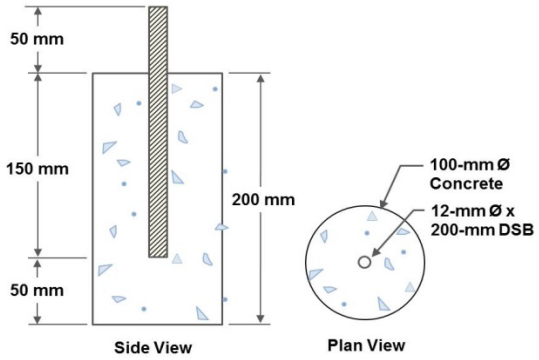

Fig. 1 Specimen's Cross-section (Left) and plan view (Right)

2.3.3 Gravimetric method

Current application lasted for 15 days. Corroded bars were extracted from cylindrical concrete and were cleaned from concrete debris. In the absence of standard cleaning solution, an attempt was made to remove the adhering rusts by exposing the samples to rust converter for a period of 2 hours.

The visible primer layer was dissolved by washing the bars with water and further cleaned by steel brushing. Cleaned bars were finally reweighed in analytical balance with 0.01g precision.

2.3.4 Impressed voltage test

Corrosion process was accelerated by impressing a constant 3-V DC to RC cylinders immersed in 3% NaCl solution. The setup was configured such that the positive terminal of power supply is connected to the embedded rebar (anode) and the negative terminal to cylindrical stainless steel (cathode) of size 8-1/2 in. high, and 6 in. diameter.

To prevent entry of oxygen to rebar-concrete junction, an epoxy coating has been applied on the said location. A 10-ohm resistor was also soldered somewhere in the protruded part of each rebar to act as the primary load of the circuit.

The current flowing through the bars was recorded using an external ammeter (data-logger) connected across the resistor (see Fig. 2) that can measure one current reading per second. Actual and schematic layout of the electrolytic cell setup is shown in Fig. 3.

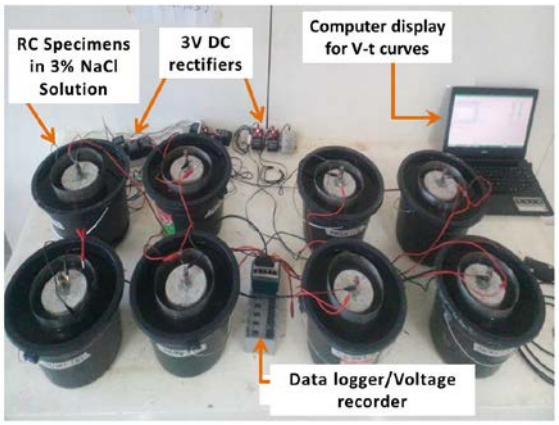

Fig. 2 Setup of impressed voltage test

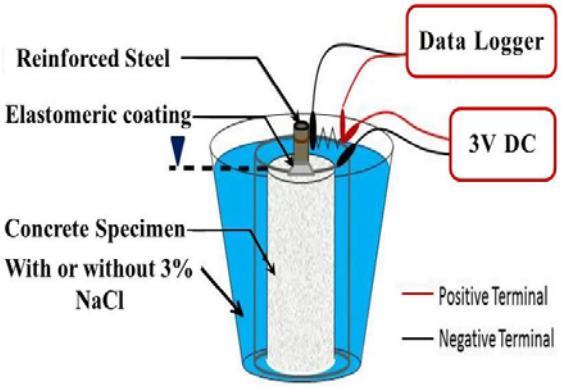

Fig. 3 Schematic of electrolytic cell per RC sample

2.4 Corrosion Damage Measurement

2.4.1 Faraday's law of electrolysis

Mass loss m (in grams) of corroded reinforcing steel can be evaluated by applying Faraday's law as shown in Eq. (1),

$$m = \frac{Qw_a}{nF} \quad (1)$$

where Q is the total charge passed, w_a is atomic molar mass (w_a= 55.847 g/mol for Fe), n is the

number of electrons transferred per iron atom ($z = 2$ for $Fe \rightarrow Fe^{2+} + 2e^{-}$), and F is the Faraday's constant parameter (F = 96,487 C/mol).

The total amount of electric charge Q resulting from electric current was calculated by getting the area under the curve of current-time relationship. Thus, the percentage of corrosion damage is given in Eq. (2),

$$C_t = \frac{m}{m_i} x100 \quad (2)$$

where m_i is the mass of original metal. The mean corrosion rate (mm/year), can be obtained as shown in Eq. (3) by rearranging the mass loss equation,

$$r = \frac{iw_a}{n\rho F} \quad (3)$$

where r is the corrosion rate, i is the corrosion current density which is the ratio of average current to the original area corroding; and w_a, n, ρ, and F as defined earlier.

Average current passed unto the bars was obtained by dividing the amount of charge liberated in Eq. (1) by the total time duration T of test as indicated in Eq. (4),

$$I_{av} = \frac{Q}{T} \quad (4)$$

2.4.2 Gravimetric method

After IVT, masses of corroded bars were weighed on an analytical balance. Mass loss is the difference in weight before and after IVT. Corrosion rate can be estimated using Eq. (5),

$$r = 8.76 * 10^4 \frac{\Delta m}{\rho A t} \quad (5)$$

where r is the corrosion rate in mm per year, Δm is the mass loss in grams, ρ is the metal density in g/cm^3, A is the surface area of steel exposed to corrosion in cm^2, and t is the exposure time in hours.

Since the steel reinforcements have changing cross-section across its length due to lugs, the density and area corroding of samples were reduced to an average value by subjecting a reference sample with same material and geometry using buoyancy test. A pre-weighed reference sample was fully submerged under water in a graduated cylinder with 2-ml precision.

From Archimedes Principle, the volume of the sample is just equivalent to the displaced volume of water. With a known embedded length, the nominal surface area under corrosion can now be obtained as summarized in Table 2.

Table 2. Measurements obtained to compute for average corroding area.

Parameter	VALUE
Gross weight (g)	172.63
Displaced Volume (cm^3)	22.00
Density (g/cm^3)	7.85
Length (cm)	20.00
Cross-sectional area (cm^2)	1.10
Average diameter (cm)	1.18
Corroding area (cm^2)	55.47

3. RESULTS AND DISCUSSION

3.1 Current-time relationship

Current values for all RC specimens generally level off at initial stage of test and may be attributed to the resistance provided by the concrete.

It was argued that the decrease is due to the temporary protection given by the passive oxide film formed at earlier stage of current application [9]. Past studies also mentioned that passivation may take effect even while concrete undergoes moist-curing [10].

Presently available chloride caused the FeOOH or FeO-layers in the passive film to break down into more porous and weaker iron-oxide (Fe2O3) [11], and thus protection lasts much faster than normal. Figure 4 shows comparison of the current values (mA) through time for all RC specimens per treatment combination.

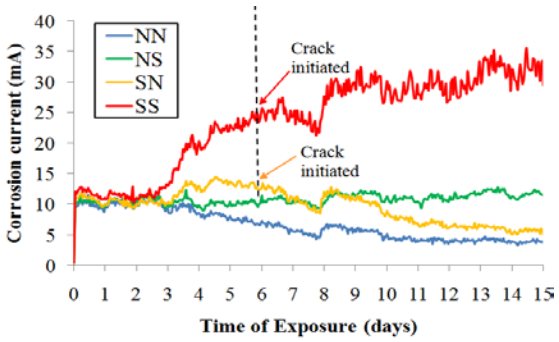

Fig. 4 Comparison of current values (mA) through time.

3.1.1 Natural-natural water combination

For the control (NN), a decline of applied current at later period indicates that concrete develops a resistive property through time. During the anodic polarization on reinforcing steel, negatively charged ions migrate into the surface of steel. With the absence of chloride, only the hydroxyl ions will be attracted in positively

polarized steel, creating an alkaline environment.

Hence, it is likely that these ions reinforced the structure of oxide passive film, which therefore suppressed the anodic reaction, i.e. $Fe \rightarrow Fe2^{+} + 2e^{-}$. This means that hydroxyls may have interacted with rebar surface eventually reducing the number of metal atoms that will undergo hydrolysis. Consequently, no cracking was observed even after 15 days of accelerated test.

3.1.2 Natural-Seawater combination

Corrosion current rises mildly as the experiment progresses, which compares well with the study of Gurdian et al [12]. Although chloride ions are indeed penetrating the concrete mass from outside as salt water saturates the sample, the corrosion is not very well active and would take place at a rate that is negligible to cause cracking.

The protection provided by the concrete bar cover may have a significant role in levelling the corrosion current even with continuous chloride ingress. The attack is also uniform due to this protection, hence allowing longer time before cracking completely initiates.

3.1.3 Seawater-Natural water combination

Current values increases, then decreases indefinitely. The observed cracks in Day ~5 are apparently due to this increase. Available chloride that has exceeded the threshold value may have reached the vicinity of rebar at a concentrated or localized nature as the attack comes directly inside the concrete mass. This caused cracking development earlier than in NS steel. However, despite the visible cracks observed, corrosion current at later times suddenly declined.

The decreasing portion can be linked to two reasons: depletion of dissolved oxygen (OH^{-}), and formation of non-conductive rust materials. Firstly, as the rate of corrosion was raised initially, the electrochemical process would in return require more oxygen for rust production. But since almost no entry point of oxygen is available, dissolved oxygen in the solution eventually becomes limited and oxygen solubility of water reduces. With appreciably no available oxygen, corrosion is impeded; thus, lowering the rate of reaction [13].

Secondly, there are no chloride ions present outside of concrete to combine with ferrous ions, which therefore prohibited further depassivation to proceed. After cracks have been induced, reinforcing steel is exposed to react for more hydroxyl ions (OH^{-}). The formed iron-oxide products, which are not as electrically conductive as the original metal, will eventually cover the rebar surface area; thus, lowering the rate of corrosion.

The trend is also a confirmation of the corrosion current behaviour recorded in control specimen (NN), both of which were immersed in chloride free water. This shows that RC structure in chloride-free water develops a resistive property, and has a tendency to slow down corrosion damage

3.1.4 Seawater-seawater combination

Onset of corrosion in SS sample is characterized by sharp increase of corrosion current values. Large amount of current flow means that corrosion is active and severe, caused by continuous passage of dissolved chlorides towards the steel surface. Expansion of oxide products resulted to tensile cracks at Day 6, allowing more chlorides to enter and further accelerating the damage. Saline water proves to exhibit deteriorating effect in RC structures when used as mixing and exposing media.

3.2 Corrosion Damage

Parameters of corrosion (percent mass loss, maximum, and average current applied) were averaged for triplicate samples and graphed in Fig. 5. The amount of current measured in IVT per treatment is also shown in Fig. 6.

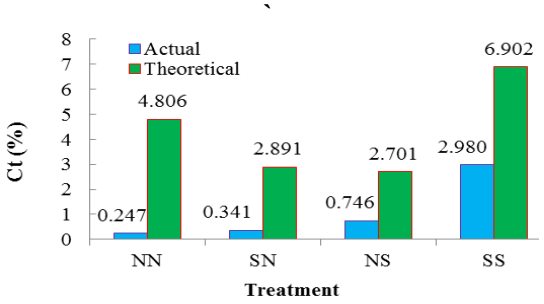

Fig. 5 Average percent corrosion

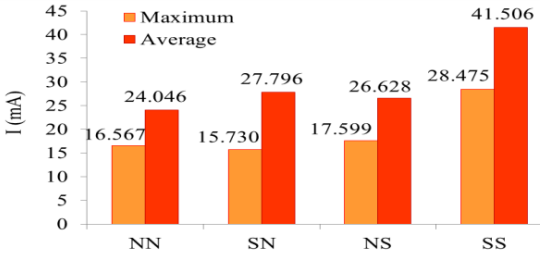

Fig. 6 Current measured in IVT per treatment.

Applied current is a measure of concrete's ability to allow flow of electrons, which is an indication of susceptibility to corrosion, while

corrosion rate measures the propagation of mass loss in steel under damage. The corrosion rate or the reaction rate of corroded reinforcement by gravimetric method is shown in Table 3. It is a matter of interest that while the control steel did not exhibit electrochemical weight loss as expected, both corrosion rate and applied current showed apparent and consistent trends.

Table 3 Reaction rate of corroded reinforcements by gravimetric method

Treatment	r (mm/yr)
NN	0.233
SN	0.323
NS	0.697
SS	2.792

The accelerated process appears to overestimate the actual damage when a weak electrolyte was used as a medium of accelerated corrosion. Discrepancy in terms of diameter loss was also reported in a separate study [14]. Complementary study suggested that other processes that competed with oxidation reaction may have been involved [15]. The inefficiency of Faraday's law was further facilitated by the alkaline, chloride-free environment that retards the same reaction, which consequently caused negligible gravimetric weight loss.

3.2.1 Time to initiate first crack

At high chloride saturation levels, anodic process will accelerate forming firm layers of hydrated ferric oxide on rebar surface at earlier stage than usual. This material expands inducing expansion pressure well above the tensile capacity of concrete. This will continue as corrosion progresses until concrete yields and cracks appear. When sufficient oxygen is present, it would lead to further chloride ingress and wider crack openings [10]. The surface conditions of RC specimens after IVT was captured and shown in Figure 7. From the image, no substantial corrosion products can be detected in the control, thus no pitting corrosion and sign of damage sustained.

On the other hand, chloride coming only from the outside (NS) does not have enough time to completely depassivate the steel, which results only to few corrosion traces. It is evident that for SN, corrosion is more active and amplified than NS. The corrosive pattern primarily concentrates in the core of concrete mass and along the rebar's length suggesting the action of chloride directly inside. Area of aggressive region in SS concrete extended from the vicinity of rebar until the surface, primarily facilitated by cracks that formed.

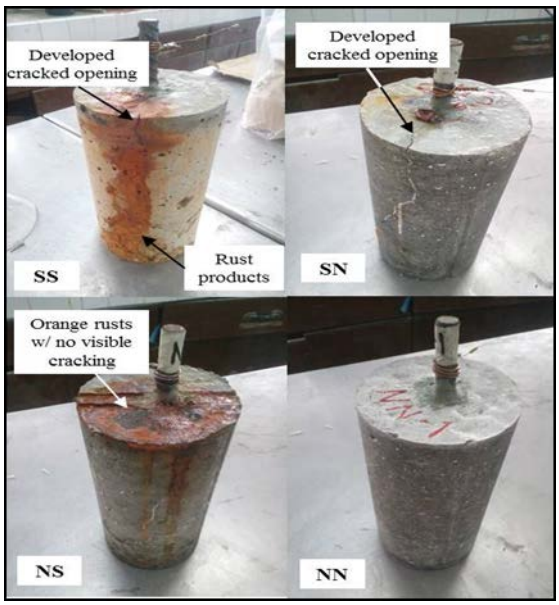

Figure 7. Concrete and steel surface observation after IVT

3.2.2 Comparison of admixing (SN) and chloride ingress (NS)

While admixing chloride (SN sample) results to more aggressive effect than chloride ingress (NS sample) due to appearance of cracks, the extent of corrosion appears more visible in NS concrete, as indicated by the trend of gravimetric mass loss. It is probably because of the trends of corrosion activity in both treatments at post-cracking stage. As an illustration, corrosion rate was computed for three samples using Faraday's law (Equation 3) before and after cracks have been observed. Since NS concrete sustained no cracks, current-time relationship was evaluated only until the latest day the cracks were observed from SN sample, i.e. day 6, the result of which is shown in Figure 8.

It can be seen that the rate of corrosion for SN concrete peaks initially, and therefore more aggressive, as the free chloride content exceeds the value necessary for depassivation [16]. This increase mainly caused the appearance of cracks in concrete. The rate then remarkably slows down after cracking due to reasons earlier discussed. On the other hand, current activity in NS concrete continuously progresses, supported by the mild but indefinite rise of current-time relationship in Figure 4. It is in this period where chloride continuously penetrates the concrete mass, which becomes more pronounced as time progresses. The rate however did not cause cracks because of uniform chloride action coming outside of concrete mass.

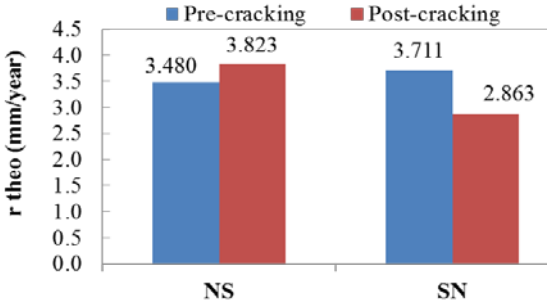

Figure 8. Average corrosion rate for NS and SN concretes before and after cracking.

3.3.3 Statistical analysis

Eight (8) sets of Single-factor ANOVA test were made in this study to test the null hypothesis (Ho) as: The presence of sodium chloride in concrete environment has no significant effect on the percent corrosion of steel; and alternative hypothesis (Ha) assuming otherwise. Table 4 shows the summary of p-values from comparisons using One-way ANOVA test for a significance level of $\alpha = 0.05$ chosen for this study.

Table 4. Summary of P-values for comparison of corrosion damage between treatments and groups

Source of variation	P-value	
	Gravity	Faraday
NN vs.NS	0.321	0.885
NN vs. SN	0.642	0.836
NN vs. SS	0.025	0.119
NS vs. SN	0.421	0.720

Overall, there is no significant difference between contaminated concrete from the control, except when compared against SS sample measured gravimetrically. This means that inclusion of seawater both inside and outside of a concrete is statistically comparable to normal concrete in terms of percent weight loss due to corrosion, which complements the work of Carancio [17], who utilized seawater curing. The observation is probably because of highly variable current activity, which resulted to non-uniform surface macrostructure after the accelerated process.

Furthermore, even as the reinforcing steel is forced to act as an anode, not all reactions are due to complete conversion of iron to rust [15]. With chloride further entering the concrete mass, non-uniform corrosion, in the form of localized pits, will most likely to occur. While this deterioration is not visible in the control steel, the effect on contaminated rebars is well pronounced. Deterioration by pitting may occupy small areas, but the damage can yield significant loss in weight of steel [10]. The magnitude, highly non-uniform in nature, may greatly vary from one steel sample to another. As in the case of SS versus NN steel by actual weighing, the difference is attributable to the severe pitting corrosion at sites accessed by excessive chloride content.

4. SUMMARY AND CONCLUSION

Real structure exposed to wet conditions may exist in either natural water or sea water environment. The objective of this study is to simulate steel corrosion in RC specimens under such conditions in an accelerated manner. This was done by applying an external constant voltage, and monitoring the corrosion current within a reasonable time period. Based on the analysis made, the following general conclusions can be drawn:

(i) Mixing seawater in reinforced concrete followed by exposure to marine environment caused severe corrosion activity, and will shortly lead to cracking; whereas, normal RC under pure water exposure was shown to exhibit passive condition.

(ii) Corrosion in normal RC exposed to seawater is not as active compared to the scenario when RC is mixed with sea water followed by exposure to normal water as indicated by absence of early cracks. However exposure longer time exposure will give relatively higher corrosion in the first scenario.

(iii) RC structure in chloride-free water develops a resistive property, and has a tendency to slow down corrosion damage.

(iv) In general, the corrosion parameters are severe in SS steel, but negligible in NN, with SN and NS having no consistent difference. The result is further supplemented by the observations made in IVT curves. Observable damage is indicative of decreased durability of concrete and ductility of steel.

(v) It is possible for weak electrolyte (i.e. pure water) to incur loss of weight in reinforcing steel under accelerated process, though barely measureable.

(vi) Theoretical prediction does not give a well-defined trend, compared to gravimetric measurement.

(vii) This study also showed that pure water solution can still induce loss of weight when accelerated corrosion is employed. However, Faraday's law becomes inefficient in estimating the damage, indicating that iron hydrolysis is not the lone reaction occurring in the anodic metal.

5. ACKNOWLEDGMENT

The authors would like to thank the Department of Civil Engineering of the College of Engineering and Agro-Industrial Technology for allowing them to use its laboratory facilities for the conduct of this research. Acknowledgement is also given to the department Laboratory Technician, Mr. Rodel Deriquito for assistance in the preparation of the specimens.

6. REFERENCES

[1] Almusallam, A. A. Effect of degree of corrosion on the properties of reinforcing steel bar. Construction and Building Materials, 15, 2001, pp.361-368.

[2] Papadopoulos, M., Apostolopoulos, C., Alexopoulos, N.D., and Pantelakis, S. Effect of Salt spray corrosion exposure on the mechanical performance of different technical class reinforcing steel bars. Material and Design, 28, 2007, pp.2318-2328. doi:10.1016/j.matdes.2006.07.017

[3] Neville, A.M. Chloride attack of reinforced concrete: an overview. Materials and Structures, 28, 1995, pp.63-70.

[4] Chess, P., and Broomfield, J. Cathodic Protection of Steel in Concrete and Masonry (2nd Ed.). Boca Raton, FL: Taylor and Francis Group, LLC, 2014.

[5] Pakshir, M., and Esmaili, S. (1998). The effect of chloride ion concentration on the corrosion of concrete. Scientia Iranica, 4(4), 1998, pp.201-205.

[6] Inazumi, S., Inazawa, T., Soralump, S., Saiki, O., and Matsumoto, H., Assessment of the Potassium Silicate Based Surface Penetration Materials with Low Viscosity in the Repair of Concrete Structures. International Journal of GEOMATE, Vol. 12, Issue 29, 2017, pp.163-170.

[7] Austin, S., Lyons, R., and Ing, M. Electrochemical behavior of steel reinforced concrete during accelerated corrosion testing. Corrosion, 60(2), 2004, pp.203-212.

[8] Malaran, S. F.J. Investigation on the corrosion resistance of concrete with recycled concrete as coarse aggregates using impressed voltage test (Unpublished Thesis Manuscript). University of the Philippines –Los Baños, PH. 2015. pp. 1-109.

[9] Morsy, S., Selim, I., and Tantawi, S. Corrosion measurements of reinforcing steel by different electrochemical techniques. Journals of Materials Science and Technology, 11, 1995, pp.447-451

[10] Song, G., and Shayan, A. Corrosion of steel in concrete: cause, detection and prediction. Vermont South, Australia: ARRB Transport Research Ltd. 1998. Pp.1-177.

[11] Williamson, J.W. Electronic Properties of Passive Films on Carbon Steel Rebar in Simulated Concrete Pore Solutions. Masteral thesis, Oregon State University, Oregon, USA. 2015. pp.1-235.

[12] Gurdian, H., Alcocel, E. G., Brotons, F., Garces, P., and Zornoza, E. (2014). Corrosion Behavior of Steel Reinforcement in Concrete with Recycled Aggregates, Fly Ash and Spent Cracking Catalyst. Materials, 7, pp.3176-3197. doi:10.3390/ma7043176.

[13] Alhozaimy, A., Hussain, R., and Al-Negheimish, A. (2016). Significance of and oxygen concentration on the quality of passive film formation for steel reinforced concrete structures during the initial curing of concrete. Cement and Concrete Composites 65, pp.171-176.

[14] Care, S., and Raharinaivo, A. Influence of impressed current on the initiation of damage in renforced mortar due to corrosion of embedded steel. Cement and Concrete Research 37(12), 2007, pp.1598-1612. doi:10.1016/j.cemconres.2007.08.022

[15] Ballim, Y., and Reid, J. (2003). Reinforcement corrosion and the deflection of RC beams - an experimental critique of current test methods. Cement and Concrete Composites 25, 2003, pp.625-632.

[16] Angst, U., and Vennesland, O. Critical chloride content in reinforced concrete - State of the Art. In M. Alexander, H. Beushausen, F. Dehn, and P. Moyo, Concrete Repair, Rehabilitation, and Retrofitting III, 2012, pp. 311-317. CRC Press.

[17] Carancio, E. M. G. Fundamental Study on the Effect of Seawater as Mixing and Curing water on Corrosion of Steel bars in concrete[Thesis Manuscript]. University of the Philippines –Los Baños, PH. 2012. pp. 1-49.